Perturbational treatment of correlation effects in the Hubbard model

G. Bulk and R. J. Jelitto

Institut für Theoretische Physik, Robert-Mayer-Strasse 8, D-6000 Frankfurt am Main 11, Federal Republic of Germany
(Received 17 May 1989; revised manuscript received 4 August 1989)

In the general frame of a modified many-body perturbation theory, the single-band Hubbard model is treated in the limit of weak electron-electron interaction. In this modification the decomposition of the Hamiltonian into an effective free system and an effective perturbation is rearranged iteratively in each order of the formalism, resulting in a successive reduction of the interaction part. In comparison with conventional perturbation techniques, this means an extended range of validity. Imposing thermodynamic self-consistency, we calculate the wave-vector-dependent electronic self-energy up to second order and analyze the influence of the Coulomb correlations. Several well-known physical properties of the Hubbard model are recovered in characteristic single-particle quantities. Therefore, the effect of the band occupation n and the electron-electron repulsion U on spectral densities, band structures, densities of states, magnetization, etc. is investigated in detail. Some of the most remarkable results are: first, a splitting of the free Bloch band into two quasiparticle subbands when the coupling strength reaches moderate values. These subbands are linked by a small damping-induced background in the density of states and are separated roughly by an energy of the order of U. In addition, the upper subband is shifted to higher energies in the spectrum proportionally to U while the lower one is nearly fixed. Second, we found a paramagnetic-ferromagnetic phase diagram that has a critical coupling strength U_c and exhibits strong indications of a lower critical occupation number n_c. There is no spontaneous magnetization in the system for parameters smaller than these values. Compared with the Stoner model, one thus obtains striking improvements. In many cases our conclusions for the weak-coupling limit are qualitatively in good agreement with well-known results in the strong-correlation regime.

I. INTRODUCTION

Much theoretical work in solid-state physics is concerned with the Coulomb interaction between electrons in conduction bands. In dealing with band magnetism or insulator-metal transitions, these electronic correlations are of exceptional significance. A realistic model to describe these phenomena was proposed some time ago independently by Gutzwiller,[1] Hubbard,[2,3] and Kanamori.[4] In the simplest case of one s band the Hamiltonian often is

$$H = H_0 + H_1$$

$$= \sum_{\mathbf{k},\sigma} [\varepsilon(\mathbf{k}) - \mu] n_{\mathbf{k}\sigma}$$

$$+ \frac{U}{N} \sum_{\substack{\mathbf{k}_1, \mathbf{k}_2 \\ \mathbf{k}_3, \mathbf{k}_4}} \delta_{\mathbf{k}_1 - \mathbf{k}_2, \mathbf{k}_4 - \mathbf{k}_3} c_{\mathbf{k}_1 \uparrow}^{\dagger} c_{\mathbf{k}_2 \uparrow} c_{\mathbf{k}_3 \downarrow}^{\dagger} c_{\mathbf{k}_4 \downarrow} . \quad (1.1)$$

The creation (annihilation) operators for electrons in Bloch states with spin σ and wave vector $\mathbf{k}$ are given by $c_{\mathbf{k}\sigma}^{\dagger}(c_{\mathbf{k}\sigma})$. The corresponding number operator is $n_{\mathbf{k}\sigma} = c_{\mathbf{k}\sigma}^{\dagger} c_{\mathbf{k}\sigma}$. Furthermore, the Hubbard parameter U characterizes the strength of the intra-atomic Coulomb interaction. μ symbolizes the chemical potential and $\varepsilon(\mathbf{k})$ are the tight-binding Bloch energies. Its center of gravity T_0 is chosen to coincide with the zero of energy. Thus the system contains only three parameters: number of electrons n per lattice site, Coulomb correlation U, and

width W of the Bloch band.

Although the Hamiltonian (1.1) surely is one of the simplest ones to incorporate the electron-electron repulsion, there are only a few exotic situations where a rigorous solution of the related many-body problem has been found.[5] Hence, before applying the model to realistic substances, it is necessary to find and understand the inherent properties of the Hamiltonian as unambiguously as feasible. It seems that the better the required approximation schemes are able to reproduce the exactly known limits, the more reliable they are. Up to our knowledge, the only formalism which interpolates reasonably well between the opposite limiting cases $W \to 0$ and $U \to 0$ is the functional integral method.[6-10] But most theories are by concept restricted to one of these situations.

In this respect the strong-correlation regime $U \gg W$ has gained a lot of interest, on one hand because there is some experimental evidence for large Coulomb matrix elements and on the other hand because it is well known that a large Hubbard U favors the existence of a magnetically ordered phase.[11] Recent scientific activities concentrate mainly on problems in heavy-fermion systems[12] and high-temperature superconductors.[13] Out of the large number of proposed approximations we merely mention as examples the Heise-Jelitto transformation[14,15] and the method of spectral moments of Nolting and co-workers.[16-19] The Heise-Jelitto transformation casts the Hubbard Hamiltonian into a form which takes correctly into account the low-energy excitations in the large-U-parameter region. This results in the proper

mean-field theory in the limit of infinite coupling strength (note: the conventional Hartree-Fock decoupling $H_1 \rightarrow (U/N)\sum_{k,q,\sigma}\langle n_{k-\sigma}\rangle n_{q\sigma}$ corresponds to the opposite extreme $U \rightarrow 0$). The major advantage of the moment method consists in the fact that neither is it of perturbation type nor has it the frequently observed arbitrariness of the decoupling of equations of motion for Green functions. Therefore it is useful in treating systems with phase transitions. Accordingly, in Refs. 16–19 a detailed discussion of the para-, ferro-, and antiferromagnetic phases of the Hubbard model is given. Compared with the phase diagram of the Stoner model the parameter regions with stable collectively ordered solutions are drastically reduced. This conclusion is not surprising, because the Stoner formalism is equivalent to a first-order U-perturbation theory which is valid only when $U \ll W$ holds.

Remarkably, up to now this limit of the parameter domain has not attracted much attention in the literature. From a physical point of view it is at least as important as the strong-correlation regime because there are some indications that bandwidth and intra-atomic Coulomb repulsion are of the same order of magnitude in the transition metals. Therefore an approach to the region $U \approx W$ from the weak-coupling limit is clearly desirable. In looking for progress beyond Hartree-Fock theory one has to mention the work of Kishore et al.,[20,21] who used a projection-operator formalism related to the theory of Mori[22,23] and obtained a second-order perturbational expression for the electronic self-energy. Presumably due to complicated Brillouin-zone summations no explicit computation was done and the importance of the correction term is unclear. Tréglia, Ducastelle, and Spanjaard[24-28] (in the following cited as TDS) also have calculated the self-energy up to U^2 for a d-band Hubbard model without intra-atomic exchange interaction. Identifying the Stoner spectrum with density-functional theory band structures, it was their intention to describe the ferromagnetic transition metals both qualitatively and quantitatively. Special emphasis was put on the treatment of nickel because it shows some significant differences between photoemission experiments[29] and band structure calculations.[30] For instance, the computed and measured d bandwidth differ by an amount of 30% and one observes a satellite structure in the density of states roughly 6 eV below the Fermi level. Although, at first glance, the TDS results seem to be convincing, we believe that the simplifications they made are too drastic to lead to reliable conclusions. This point of view is clearly supported by a recently published letter of Taranko, Taranko, and Malek[31] who used a much improved version of the TDS formalism. We shall come back to these points in some detail on discussing our results later on.

Kleinman and Mednick,[32,33] too, found the same second-order expression for the self-energy and discussed its application to ferromagnetic Ni. If one reduces—by a suitable choice of parameters—the extended single-band Hubbard model dealt with by Taranko and Taranko[34] to the standard Hamiltonian (1.1), their term also corresponds to the second-order self-energy. The main disadvantage of these theories, and similarly of the TDS work,

is the lack of (thermodynamic) self-consistency.

In the present paper we propose a generally applicable many-body perturbation theory which works on the basis of the standard procedures but uses a modified partitioning of the Hamiltonian. Its single-particle analogue and applications to some simple problems are described elsewhere.[35] The details of the iterated decomposition of the Hamiltonian will be explained in Sec. II. In Sec. III the formalism is used to calculate the single-particle properties of the s-band Hubbard model (1.1). We find that the self-energy in second-order modified perturbation theory (MPT) interpolates in a very reasonable manner between standard and self-consistent perturbation formalisms without requiring the large numerical computational effort of the latter. Sec. IV discusses the thermodynamically self-consistent solutions of the MPT. We compare the results with those of standard procedures with special emphasis to possible satellite structures and their physical significance. A systematic analysis of the paramagnetic region reveals for a certain parameter range a splitting of the Stoner excitations into two well-defined quasiparticles. This splitting persists into the region of ferromagnetic solutions which were also found. A phase diagram for para- versus ferromagnetism is constructed and compared with Hartree-Fock results.

Whether other collectively ordered structures, as for example $ABAB$ antiferromagnetism, are possible or not has to be left to further investigations and shall not be addressed in this paper.[36]

II. PERTURBATION THEORY WITH ITERATED PARTITIONING OF THE HAMILTONIAN

In solving the Dyson equation for the single-particle Green function,

$$G_{k\sigma}(z) = \frac{\hbar}{\hbar z - \varepsilon(k) + \mu - \Sigma_{k\sigma}(z)} , \qquad (2.1)$$

one generally has to make approximations because the interaction part of a physically realistic Hamiltonian leads in almost every case to a self-energy $\Sigma_{k\sigma}(z)$ which cannot be calculated exactly. In a perturbational treatment of this self-energy, in contrast to breaking off the Dyson series,

$$G_{k\sigma}(z) = \langle k\sigma | (\hbar z - H_0 - H_1)^{-1} | k\sigma \rangle$$
$$= \langle k\sigma | G_0 + G_0(H_1/\hbar)G_0$$
$$+ G_0(H_1/\hbar)G_0(H_1/\hbar)G_0 + \cdots | k\sigma \rangle ,$$
$$(2.2)$$

$$G_0 = G_0(z) = \hbar(\hbar z - H_0)^{-1} , \qquad (2.3)$$

after a finite number of steps, one has already completely summed up some partial series of (2.2).

For example, using conventional perturbation theory (CPT) the self-energy is expanded in powers of H_1:

$$\Sigma_{k\sigma}(z) = \sum_{n=1}^{\infty} \Sigma_{k\sigma}^{(n)}(z), \quad \Sigma_{k\sigma}^{(n)} = \Sigma_{k\sigma}^{(n)}[G_0] . \qquad (2.4)$$

In each order the term $\Sigma^{(n)}$ depends only on the matrix elements of the interaction and is a functional of the free

propagator G_0. Then, normally, the exact Green function is calculated up to an order N:

$$G_{k\sigma}^{(N)}(z) = \frac{\hbar}{\hbar[G_{k\sigma,0}(z)]^{-1} - \sum\limits_{n=1}^{N} \Sigma_{k\sigma}^{(n)}(z;[G_0])} . \quad (2.5)$$

In an alternative procedure, called self-consistent perturbation theory, the self-energy contributions are taken to be functionals of the full propagator. But then one has to take into account the so-called skeleton terms only in order to avoid multiple counting of some contributions:

$$\Sigma_{k\sigma}(z) = \sum\limits_{n=1}^{\infty} \tilde{\Sigma}_{k\sigma}^{(n)}(z), \quad \tilde{\Sigma}_{k\sigma}^{(n)} = \tilde{\Sigma}_{k\sigma}^{(n)}[G] . \quad (2.6)$$

Now, computing the Nth order approximation of the Green function, far more partial sums of (2.2) are incorporated:

$$G_{k\sigma}^{(N)}(z) = \frac{\hbar}{\hbar[G_{k\sigma,0}(z)]^{-1} - \sum\limits_{n=1}^{N} \tilde{\Sigma}_{k\sigma}^{(n)}(z;[G^{(N)}])} . \quad (2.7)$$

Whether such perturbation expansions are convergent, and whether the necessary rearrangements of special partial series are allowed, are mathematically difficult problems and yet unanswered for many physical systems. We have no intention to address this matter, but let us state that the MPT will surely converge if the CPT does.

It is worth noting that in each of the expansions (2.5) and (2.7) for the Nth order approximation the preceding $N - 1$ orders occur only in the form of additive terms. We want to take advantage of this fact in order to use the lower steps as effectively as possible for computing the self-energy of the Nth order. To achieve this goal, the following iterative partitioning of the Hamiltonian into an effective free system and an effective perturbation is adopted:

$$H = H_0^{(N)} + H_1^{(N)} , \quad (2.8)$$

$$N = 1: \quad H_0^{(1)} = H_0, \quad H_1^{(1)} = H_1 , \quad (2.9)$$

$$N > 1: \quad \begin{cases} H_0^{(N)} = H_0^{(N-1)} + V^{(N-1)}(z) , & (2.10) \\[4pt] H_1^{(N)} = H - H_0^{(N)}(z) , & (2.11) \\[4pt] V^{(N-1)}(z) = \sum\limits_{k,\sigma} M_{k\sigma}^{(N-1)}(z) n_{k\sigma} , & (2.12) \end{cases}$$

where $M_{k\sigma}^{(N-1)}(z)$ is the sum of all self-energy contributions up to the order $N - 1$ calculated with respect to the decomposition into $H_0^{(N-1)}$ and $H_1^{(N-1)}$.

Although now after every partitioning a perturbation theory of arbitrary order larger than $N - 1$ might be performed, we believe a better way is to repeat the iteration process (2.10)–(2.12) already after the Nth step has been carried out. This makes for an optimal reduction of the perturbation. At this level the "free" propagator is just the full propagator of the preceding order:

$$G_{k\sigma,0}^{(N)}(z) = \frac{\hbar}{\hbar[G_{k\sigma,0}^{(N-1)}(z)]^{-1} - M_{k\sigma}^{(N-1)}(z)} . \quad (2.13)$$

When the modified formalism is based on the conventional expansion (2.5) one quickly recognizes that it yields improved results. On one hand this is due to the more realistic effective undisturbed Green function which is much closer to the exact one than the original zeroth approximation (2.3). In addition, the successive renormalization of the interaction operator on the other hand leads to an ever decreasing perturbation.

If, in comparison, the self-consistent perturbation theory (2.7) is taken as the starting point for the modified procedure no progress in the quality of $G_{k\sigma}^{(N)}$ is attainable. This is because the unperturbed Green function (2.13) is cancelled by the contribution $n = 1$ of the expansion (2.6) and therefore does not occur explicitly in the representation (2.7). Furthermore the iterated interaction operator cannot create other skeletons than H_1 itself. Nevertheless one has to keep in mind that there are only very few cases of low order where the terms of self-consistent perturbation theory can actually be calculated. In those situations the effective free propagator (2.13) will turn out to be a much more suitable starting point for an iteration scheme to obtain the solution of (2.7) than the original one (2.3). Due to the complicated structure of the self-energy terms it is generally not possible to iterate the equations until convergence has been achieved, and one has to stop after a few steps. Then taking (2.13) as the zeroth approximation, of course one will again obtain better results.

Physically $H_0^{(N)}$ describes a system of quasiparticles with excitation energies $\varepsilon_\sigma(k)$ resulting from the equation

$$\varepsilon_\sigma(k) = \varepsilon(k) - \mu - \mathrm{Re}\left[\sum\limits_{n=1}^{N-1} M_{k\sigma}^{(n)}[\varepsilon_\sigma(k) + i0^+] \right] \quad (2.14)$$

and lifetimes $\tau_{k\sigma}$ according to

$$\tau_{k\sigma} = \hbar \frac{\left| 1 - \dfrac{\partial}{\partial E}\left[\mathrm{Re}\left[\sum\limits_{n=1}^{N-1} M_{k\sigma}^{(n)}(E + i0^+) \right] \right] \right|_{E = \varepsilon_\sigma(k)}}{\left| \mathrm{Im}\left[\sum\limits_{n=1}^{N-1} M_{k\sigma}^{(n)}[\varepsilon_\sigma(k) + i0^+] \right] \right|} . \quad (2.15)$$

The renormalized perturbation $H_1^{(N)}$ mediates an interaction between these quasiparticles.

In an explicit expansion of the self-energy, for instance in the framework of the Feynman diagram technique, the z dependence of the effective operators has to be treated in the same way as that of the free propagator G_0. The fact that $H_0^{(N)}$ and $H_1^{(N)}$ are no longer Hermitean operators does not cause any problems as far as the applicability of perturbation theory is concerned.

Finally it has to be remarked that convergence of the MPT may be achieved already after a few orders due to the successively renormalized perturbation. Therefore it is also reasonable to expect an extended range of validity covering the region of moderate- or even strong-coupling parameters (which is confirmed by the examples in Ref. 35). After all, compared with the standard procedure, the supplementary computational and numerical effort is relatively small. This is because the self-energy terms of

the preceding $N-1$ orders have to be calculated anyway and therefore are available for the Nth step.

III. COULOMB CORRELATIONS IN THE HUBBARD MODEL

Before one can analyze the many-body problem of electron-electron correlations in the s-band Hubbard model by means of the MPT, first of all a method for an explicit determination of the self-energy contributions has to be chosen. In contrast to the method of Feynman graphs used so frequently in the literature, here an alternative procedure based on the Mori formalism[22,23] is employed.

In the Liouville space $\mathcal{L}$, for any observable A and scalar product $(\cdot|\cdot)$ there holds the identity

$$\frac{(A|A)_z}{(A|A)} = \frac{i}{z - \Omega + i\gamma(z)} .$$ (3.1)

The correlation function $(A|A)_z$ is the one-sided Fourier transform of $(A(t)|A)$,

$$(A|A)_z = \int_0^\infty dt\, e^{izt}(A(t)|A)\quad (\text{Im}(z) > 0) .$$ (3.2)

Ω is the characteristic frequency of the system,

$$\Omega = (A|LA)\frac{1}{(A|A)} ,$$ (3.3)

and $\gamma(z)$ denotes the memory function,

$$\gamma(z) = \left(QLA\left|\frac{i}{z - QLQ}\right|QLA\right)\frac{1}{(A|A)} ,$$ (3.4)

where the Liouville Operator L was introduced,

$$L|X) = \frac{1}{\hbar}|[H,X]_-)\quad \forall|X)\in\mathcal{L} ,$$ (3.5)

as well as a projection operator Q, projecting onto the orthogonal complement of the linear space $\mathcal{L}_A$ spanned out by $|A)$,

$$Q = 1 - |A)\frac{1}{(A|A)}(A| .$$ (3.6)

A decomposition of the Hamiltonian H induces a partitioning of the Liouville operator

$$L = L_0 + L_1 .$$ (3.7)

If L_0 keeps the subspace $\mathcal{L}_A$ invariant,

$$L_0|Y)\in\mathcal{L}_A\quad \forall|Y)\in\mathcal{L}_A ,$$ (3.8)

a perturbation expansion of $(A|A)_z$ in terms of powers of L_1 is possible. Because of the relation

$$QL|A) = QL_1|A)$$ (3.9)

such an expansion for the memory function just starts with a second-order term.

In the present work we want to carry out the MPT up to and including this contribution. Therefore higher terms of the memory function are not needed. For the scalar product we work with the thermodynamical expectation value of the anticommutator,

$$(X|Y) = \langle[X^\dagger,Y]_+\rangle ,$$ (3.10)

and hence have the following simple relationship with the retarded anticommutator Green function:

$$\langle\langle A^\dagger; A\rangle\rangle_z^{\text{ret}} = -i(A|A)_z .$$ (3.11)

Now indicating with a lower subscript zero an evaluation of thermodynamical averages with respect to the free system for the second-order term of the memory function (3.4) there remains only

$$\gamma_2(z) = \left(Q_0L_1A\left|\frac{i}{z - L_0}\right|Q_0L_1A\right)_0\frac{1}{(A|A)_0} ,$$ (3.12)

where we have used

$$Q_0L_0Q_0|X)_0 = L_0Q_0|X)_0 .$$ (3.13)

Finally inserting the electron creation operator $c_{k\sigma}^\dagger$ for the observable A, one finds

$$G_{k\sigma}(z) = -i(c_{k\sigma}^\dagger|c_{k\sigma}^\dagger)_z ,$$

$$\Sigma_{k\sigma}(z) = \hbar\Omega_{k\sigma} - \varepsilon(k) + \mu - i\hbar\gamma(z) .$$ (3.14)

In detail, using (1.2) one obtains

$$Lc_{k\sigma}^\dagger = \frac{1}{\hbar}\left[[\varepsilon(k) - \mu]c_{k\sigma}^\dagger + U\frac{1}{N}\sum_{q,p}c_{q\sigma}^\dagger c_{p-\sigma}^\dagger c_{q+p-k-\sigma}\right]$$ (3.15)

and

$$\Omega_{k\sigma} = \frac{1}{\hbar}[\varepsilon(k) + Un_{-\sigma} - \mu] ,$$ (3.16)

where we have introduced

$$n_{-\sigma} = \langle n_{i-\sigma}\rangle\quad \forall i$$ (3.17)

because of the assumed translational symmetry. Up to the first order the Hartree-Fock approximation is reproduced,

$$(c_{k\sigma}^\dagger|c_{k\sigma}^\dagger)_{z,1} = \frac{i\hbar}{\hbar z - \varepsilon(k) - Un_{-\sigma}^{(1)} + \mu} ,$$ (3.18)

which has to be solved self-consistently. Therefore, with

$$\Sigma_{k\sigma}^{(1)}(z) \equiv Un_{-\sigma}^{(1)} = U_{-\sigma} ,$$ (3.19)

an appropriate first decomposition of the Hamiltonian following (2.8)–(2.12) is given by

$$H_0^{(2)} = H_0 + \sum_{k,\sigma}U_{-\sigma}n_{k\sigma} ,$$

$$H_1^{(2)} = H_1 - \sum_{k,\sigma}U_{-\sigma}n_{k\sigma} .$$ (3.20)

It should be noted that now the possibility of a magnetic phase transition is incorporated already in the free system. Hence it is an intrinsic property of a perturbation formalism based on the partitioning (3.20).

Moving up to the next order the characteristic frequency $\Omega_{k\sigma}$ still obeys the exact relation (3.16). A lengthy but simple calculation leads to

$$(L_0^{(2)})^n[Q_0^{(2)}L_1^{(2)}|c_{\mathbf{k}\sigma}^\dagger\rangle_0^{(2)}]=\frac{-1}{\hbar^{n+1}}\{U_{-\sigma}[\varepsilon(\mathbf{k})+U_{-\sigma}-\mu]^n|c_{\mathbf{k}\sigma}^\dagger\rangle_0^{(2)}$$

$$-U\frac{1}{N}\sum_{\mathbf{q},\mathbf{p}}[\varepsilon(\mathbf{q})+\varepsilon(\mathbf{p})-\varepsilon(\mathbf{q}+\mathbf{p}-\mathbf{k})+U_{-\sigma}-\mu]^n|c_{\mathbf{q}\sigma}^\dagger c_{\mathbf{p}-\sigma}^\dagger c_{\mathbf{q}+\mathbf{p}-\mathbf{k}-\sigma}\rangle_0^{(2)}\} \quad . \quad (3.21)$$

Calculating the remaining inner products in the effective free system, which is again tedious but without serious problems, and introducing the abbreviation

$$f_{\mathbf{p}\sigma}=\langle n_{\mathbf{p}\sigma}\rangle_0^{(2)}=\frac{1}{\exp\{\beta[\varepsilon(\mathbf{p})+U_{-\sigma}-\mu]\}+1} \tag{3.22}$$

the second-order memory function may be cast into the form

$$\gamma_2^{(2)}(z)=\frac{i}{\hbar}U^2\frac{1}{N^2}\sum_{\mathbf{q},\mathbf{p},\mathbf{r}}\delta_{\mathbf{r}+\mathbf{k},\mathbf{q}+\mathbf{p}}\frac{(1-f_{\mathbf{q}\sigma})(1-f_{\mathbf{p}-\sigma})f_{\mathbf{r}-\sigma}+f_{\mathbf{q}\sigma}f_{\mathbf{p}-\sigma}(1-f_{\mathbf{r}-\sigma})}{\hbar z-\varepsilon(\mathbf{q})-\varepsilon(\mathbf{p})+\varepsilon(\mathbf{r})-U_{-\sigma}+\mu} \quad . \tag{3.23}$$

The first term describes the scattering of an incoming Hartree-Fock electron $(\mathbf{k},\sigma)$ with another one $(\mathbf{r},-\sigma)$ into the empty electron states $(\mathbf{q},\sigma)$ and $(\mathbf{p},-\sigma)$. In the same way the second part refers to hole-hole scattering.

When, for the moment, we consider only the sum of the Fermi functions in (3.23) it can be seen that the memory function scales roughly like

$$\gamma_2^{(2)}\propto n_{-\sigma}(1-n_{-\sigma})U^2 \quad . \tag{3.24}$$

Consequently the region of validity of the MPT is further extended when the electron or hole concentration in the system is small.

Although strictly spoken there may be doubts concerning the reliability of the perturbational method, formally there are no problems when the Hubbard parameter U becomes large. Then $\gamma_2^{(2)}$ grows linearly with coupling strength. Hence the physical properties which can be derived from the one-particle propagator in (3.14) should approximately develop proportional to U. This conclusion is borne out by theories worked out for the strong-coupling limit[16-19] whose single-particle quantities all scale linearly with U.

For further practical evaluation of (3.23) the Kronecker δ is expanded in a Fourier series and the Brillouin-zone (BZ) summations are replaced by energy integrations:

$$\gamma_2^{(2)}(z)=\frac{i}{\hbar}U^2\sum_i e^{i\mathbf{k}\cdot\mathbf{R}_i}\int\int_{-\infty}^{\infty}\int dE_1dE_2dE_3\rho_i(E_1)\rho_i(E_2)\rho_i(E_3)\cdot\frac{(1-f_{1\sigma})(1-f_{2-\sigma})f_{3-\sigma}+f_{1\sigma}f_{2-\sigma}(1-f_{3-\sigma})}{\hbar z-E_1-E_2+E_3-U_{-\sigma}+\mu} \quad . \tag{3.25}$$

The abbreviations

$$f_{j\sigma}=\frac{1}{\exp[\beta(E_j+U_{-\sigma}-\mu)]+1} \quad , \tag{3.26}$$

$$\rho_i(x)=\frac{1}{N}\sum_{\mathbf{p}\in\mathrm{IBZ}}e^{i\mathbf{p}\cdot\mathbf{R}_i}\delta(x-\varepsilon(\mathbf{p})) \tag{3.27}$$

are used. Thus the sixfold summation of (3.23) is replaced by a lattice sum connected with a threefold integration for each term. Also it is necessary to evaluate the auxiliary quantities ρ_i which themselves depend only on the distance of a lattice site from the origin. Therefore (3.25) may be written as a sum over all neighboring spheres n with radius δ_n:

$$\gamma_2^{(2)}(z)=\sum_n\gamma_{\mathbf{k}\sigma,n}(z) \quad . \tag{3.28}$$

In accordance with the tight-binding approximation of the electron hopping we shall assume that the contributions become quickly smaller with growing distance δ_n and that it is sufficient to keep the local term with $n=0$ and among the nonlocal contributions only the term with $n=1$. For the origin $\mathbf{R}_i=0$ (3.27) is just the free Bloch density of states ρ_0. Using the expressions given in Ref. 37 for this function, one can calculate analytically the

Hilbert transform of ρ_0 which is required for an explicit numerical evaluation. Because any nearest-neighbor (NN) site $\mathbf{R}_{\mathrm{NN}}$ results in the same ρ_1, we have for a simple-cubic lattice

$$\rho_1(x)=\frac{1}{N}\sum_{\mathbf{p}}\left[\frac{1}{6}\sum_{\mathrm{NN}}e^{i\mathbf{p}\cdot\mathbf{R}_{\mathrm{NN}}}\right]\delta(x-\varepsilon(\mathbf{p}))$$

$$=-\frac{2}{W}x\rho_0(x) \quad . \tag{3.29}$$

Then there remains

$$\gamma_2^{(2)}(z)=\gamma_{\sigma,0}(z)+\varepsilon(\mathbf{k})\gamma_{\sigma,1}(z)$$

$$=\frac{i}{\hbar}[\Sigma_{\sigma,0}(\hbar z+\mu)+\varepsilon(\mathbf{k})\Sigma_{\sigma,1}(\hbar z+\mu)] \quad . \tag{3.30}$$

From this, the spectral density

$$A_{\mathbf{k}\sigma}(E)=\frac{1}{\pi\hbar}\mathrm{Im}[i(c_{\mathbf{k}\sigma}^\dagger|c_{\mathbf{k}\sigma}^\dagger)_{z=(1/\hbar)(E-\mu)+i0^+}] \tag{3.31}$$

and the quasiparticle density of states (QDOS)

$$\rho_\sigma(E)=\frac{1}{N}\sum_{\mathbf{k}}A_{\mathbf{k}\sigma}(E) \tag{3.32}$$

are easily obtained.

For a given set of parameters, consisting of Bloch bandwidth W, Coulomb repulsion U, and average electron number n per lattice site, we calculate the quasiparticle occupation numbers n_σ and the chemical potential μ in a *thermodynamically self-consistent* scheme by solving the two equations:

$$n_\sigma = \int_{-\infty}^{\infty} dE \frac{\rho_\sigma(E)}{\exp[\beta(E-\mu)]+1} \quad \sigma \in \{\uparrow,\downarrow\} \ . \quad (3.33)$$

The self-consistency requirement means replacing $U_{-\sigma}$ by $Un_{-\sigma}$ in all equations.

Finally we point out that the Hubbard model can be rescaled with the Bloch bandwidth W, i.e., the proper coupling parameter is U/W. For this reason we have renormalized all energy quantities that occur; spacings in energy of magnitude 1 now correspond to the full Bloch bandwidth W.

The equations (3.33) are solved numerically at the absolute zero of temperature $T=0$ K. The results obtained are discussed in the following section.

IV. DISCUSSION OF RESULTS

A. Comparison with conventional procedures

The previous work on second-order perturbation theory[24-28,32,33] was mainly carried out for a quantitative description of the transition metals, especially nickel. We are interested in a qualitative analysis of the Hubbard model, which is why explicit comparison is possible with Ref. 24 only. In that publication, however, some supplementary assumptions and simplifications were made, which can be summed up as follows: (a) The Bloch energies of the free system already incorporate the Stoner corrections and may be identified with the results of single-particle band-structure calculations. (b) The nonlocal terms of the second-order self-energy [i.e., $n \geq 1$ in (3.28)] are small compared with the local one and may be neglected. (c) The dependence of the results on the band-structure of the free system is not very significant, so that a rectangular free Bloch density of states was adopted. (d) The calculations are (thermodynamically) non-self-consistent (i.e., particle number and Fermi level are treated as independent variables).

We believe that each of these restrictions has a significant influence on the results. The lack of self-consistency has recently been removed by Taranko, Taranko, and Malek.[31] In the weak-U limit their findings represent a distinct improvement in comparison with TDS.

In what follows in this subsection we restrict our considerations to the paramagnetic phase and to the half-filled band $n=1$ because for symmetry reasons the shortcomings of a non-self-consistent calculation are not as serious as for other electron occupation numbers. Later on the thermodynamically self-consistent results calculated by the MPT will also be given for different values of n. Henceforth the term "self-energy" will always denote the second-order contribution of the expansion of (3.14).

Figure 1 shows the imaginary (a) and the real part (b)

of the self-energy. Both the CPT [which may be obtained from (3.33) with $U_\sigma=0$] and the MPT are calculated using the correct tight-binding density of states for a simple-cubic crystal and a $\mathbf{k}$ dependence of the self-energy according to (3.30). In the framework of a perturbation formalism the choice of $U=0.6$ corresponds to a realistic value. Plotted are the curves for $\mathbf{k}=\frac{1}{2}(1,1,1)$ because then the nonlocal term vanishes and a direct comparison with the TDS self-energy is possible.

First of all one finds characteristic regions where the damping is nonzero. Because of the starting point (3.20) of the MPT the imaginary part is shifted by the linear Stoner correction $Un_{-\sigma}$. It is strongly energy dependent in all three variants indicating correspondingly strong deviations of the spectral density from a Lorentzian. Furthermore in the immediate vicinity of the Fermi level the damping is proportional to $(E-\mu)^2$ as is predicted by the general Landau theory of Fermi liquids. The antisymmetry and symmetry, respectively, of the real and imaginary part in TDS and MPT reflect the particle-hole
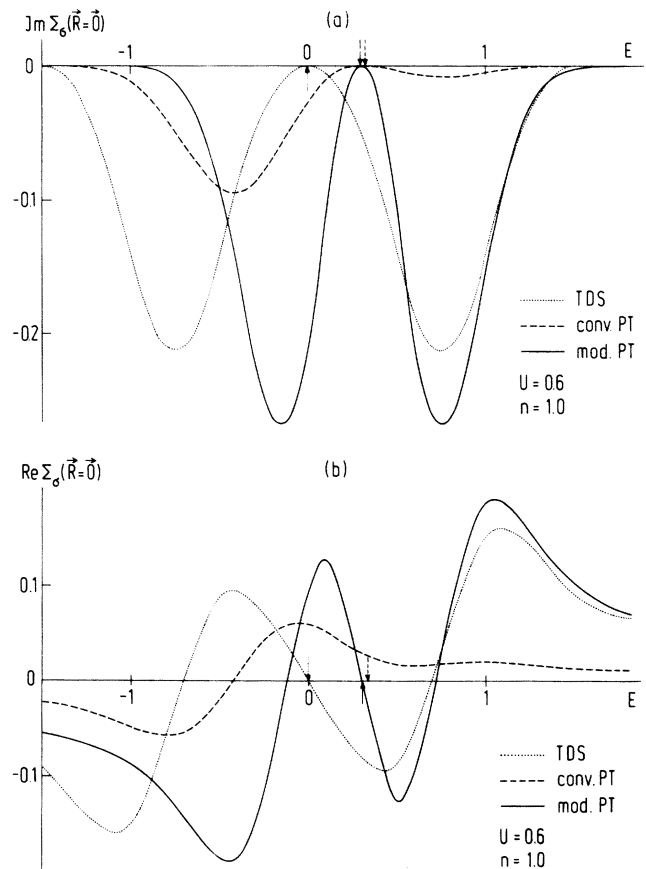

FIG. 1. Imaginary part (a) and real part (b) of the local contribution of the electronic self-energy (= second-order term of the self-energy) calculated by different methods: Dotted curve: analogous to TDS; dashed curve: conventional perturbation theory; solid curve: modified perturbation theory. The arrows indicate the Fermi level of the corresponding method. Other parameters are given in the figure.

symmetry of the half-filled band. Using CPT, the chemical potential is shifted in rough proportion to the paramagnetic Stoner contribution $\frac{1}{2}Un$ making for a nonsymmetric self-energy. In order to avoid this behavior, $\frac{1}{2}Un$ must not become large. This is why the ordinary perturbation formalism yields reasonable results only for very weak U.

The importance of choosing the correct free density of states becomes particularly clear in the quantitative differences of the damping maxima. In the TDS version they lie clearly outside the range of the free band. At the band edges the damping reaches only half the maximum value. In contrast to this in the MPT the regions of extremal imaginary part coincide with the edges of the original Stoner band. Thus, states lying there are maximally damped. Moreover, our formalism clearly produces higher maximum values. Hence, due to the Coulomb correlations, those Stoner quasiparticles with extremal excitation energies are strongly broadened. Therefore a narrowing of the width of the Stoner band will result.

This impression is strengthened by the graph of the real part which characterizes the shift of Hartree-Fock excitations. Again our curves show more structure than TDS ones. The MPT shift is small at the edges of the Stoner band and becomes comparatively large in the center of its upper and lower half, respectively. This leads to a further reduction of the bandwidth. In contrast, the band narrowing in the TDS formalism is caused merely by a displacement of states with extremal energy into regions where they are strongly broadened. All in all

one expects pronounced additional structure in the QDOS below and above the domain of the Hartree-Fock excitations which contracts with increasing electron repulsion.

When U exceeds the magnitude of the bandwidth the self-energy roughly scales—as was already mentioned—with U. So the downward displacement of states has to be compared with the shift proportional to $\frac{1}{2}Un$ of the whole spectrum towards higher energies. There is a good chance that these two effects almost compensate each other leading to a nearly U-independent structure. On the other hand there are also states which are shifted upwards amplifying the Stoner displacement already present. Hence the resulting structure will move in proportion to U but with a proportionality factor larger than the $\frac{1}{2}n$ of the Hartree-Fock band.

Finally there are states in the neighborhood of the Fermi level which are broadened and shifted only weakly. This results in an additional peak in the QDOS in the central region of the original Stoner band. But this is only true for the half-filled band due to its special symmetry. The imaginary part is nonsymmetric with reference to the chemical potential for any $n \neq 1$ (see, for example, Fig. 4). In that case the shift of states is comparatively large where the damping is small, so that no central structure will occur.

Calculating the spectral density $A_{\mathbf{k}\sigma}$ for the MPT self-energies leads to a sharp peak because for $\mathbf{k} = \frac{1}{2}(1,1,1)$ the corresponding excitation energy coincides with the Fermi level, i.e., is undamped. $A_{\mathbf{k}\sigma}$ is plotted in Fig. 2 as
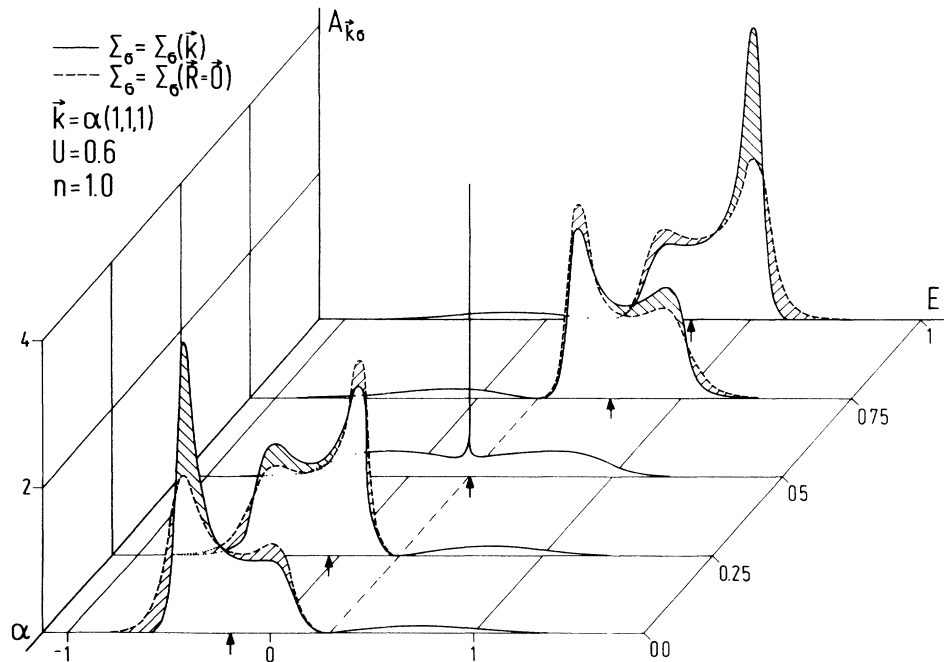

FIG. 2. Spectral density $A_{\mathbf{k}\sigma}$ as function of energy for different $\mathbf{k}$ points in the Γ-R direction of the simple-cubic Brillouin zone. Dashed curves correspond to calculations which were done using the local part of the self-energy only. The solid curves belong to the full self-energy. The influence of the $\mathbf{k}$ dependence is emphasized by hatched areas. Here the arrows label the positions of the undamped Stoner excitations. Remaining parameters are given in the plot.

a function of energy for different **k** points in the Γ-R direction (the wave vector **k** is defined by a parameter α according to $\mathbf{k}=\alpha(1,1,1)$, $\Gamma=(0,0,0)$, $R=(1,1,1)$). The hatched areas, corresponding to differences in the calculations with (solid line) and without (dashed line) the non-local part of the self-energy, clearly emphasize the necessity of including wave-vector effects on the self-energy. There is a drastic effect in the lifetime of the excitations which are identified as narrow peaks in the spectral densities. It has to be stressed that their positions are shifted with respect to the Stoner excitations, which are indicated by arrows. The striking wave-vector dependence and structure of the curves, which strongly deviates from Lorentzians, is clearly due to the behavior of the real and imaginary part of the self-energy as a function of **k** and E. The damping and the shift of states show a considerable **k** dispersion being responsible for the hatched domains.

There is good qualitative agreement with Ref. 34, where the memory function (3.23) has been calculated non-self-consistently using a Monte Carlo integration procedure for the multiple wave-vector summations. The authors point out that the **k** dependence of the self-energy and hence the spectral density is most prominent at the Γ point whereas it is rather unimportant in the "middle" of the Brillouin zone. In the light of formula (3.30) this is easily intelligible because at the Γ point $\varepsilon(\mathbf{k})$ is extremal and in the "middle" of the zone it is relatively small. On the other hand one may conclude therefrom that the parametrization chosen for the **k** dependence works very reliably.

All trends derived in the discussion above are corroborated by the QDOS. This quantity is shown in Fig. 3, computed by different methods. In each part (a), (b), and

(c) the Hubbard parameter varies between 0.0 and 0.9 bandwidths. As soon as the Coulomb correlation is switched on, the QDOS is broadened overall within the region of nonvanishing damping. When the electron-electron interaction is small, one observes only an additional flattening of the van Hove singularities in the original density of states.

From part (a) of Fig. 3 one may analyze the influence of U in the framework of the TDS method.[24] In the region of moderate coupling strength ($0.5 \lesssim U \lesssim 1.0$) the form of the density of states is altered drastically. Besides a pronounced narrowing of the central peak there occur two shoulders at the wings of the original band. The authors believe that the lower shoulder is due to hole excitations and the upper one due to electron excitations with final states which in each case are localized at a single site. They then proceed to interpret the single lower shoulder, which only survives when they insert a band filling adequate for nickel, as the 6 eV satellite seen in the photoemission spectra of Ni.

We disagree with this explanation and believe that some modifications are necessary. In our opinion, which is founded on part (c) and a more detailed analysis given in Sec. IV B, the two satellites occurring in the regime of moderate and strong U have to be identified with the two subbands of the Hubbard model. It is generally believed that due to the Coulomb interaction the free Bloch band with center of gravity T_0 splits into two quasiparticle subbands about T_0 and T_0+U when U is large. Particularly for $U=0.9$ in Fig. 3(c) the new bands are evident. The lower one consists of electrons which preferentially hop via empty lattice sites whereas in the upper subband propagation is more likely to proceed via sites where another electron with opposite spin is already present and
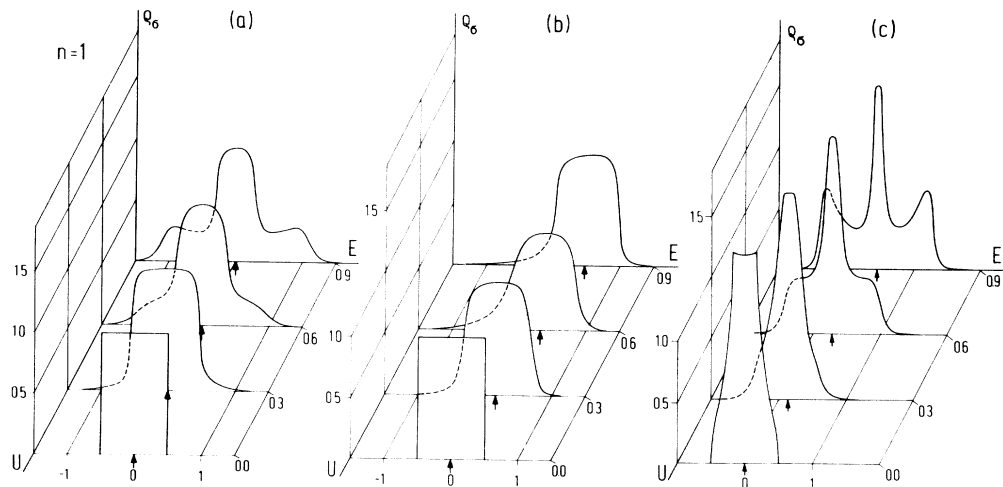

FIG. 3. Paramagnetic quasiparticle density of states in terms of energy for several U values in the case of the half-filled band: (a) non-self-consistent TDS-method; (b) thermodynamically self-consistent CPT (with **k** dependent self-energy); (c) thermodynamically self-consistent MPT (with **k** dependent self-energy). In (a) and (b) a rectangular density of states is used whereas in (c) the correct Bloch density of states was employed. The position of the Fermi level is indicated by an arrow.

therefore an additional energy U is needed.

As already mentioned in discussing the self-energy there remains in the symmetric situation $n = 1$ a third band in the region of the original Stoner density of states. This somewhat unphysical structure, which is a residue of the mean-field theory taken as the first approximation, should disappear as soon as the number of electrons deviates from half filling. Furthermore, going up to higher values of the Hubbard parameter, for which we did not plot the curves here, the weight of the central peak decreases drastically compared with that of the upper and lower subband. These two become more and more dominant, always having equal weight and being roughly situated at energies zero and U, respectively.

The QDOS in Fig. 3(b) was calculated using a rectangular density of states and wave-vector-dependent self-energies in the frame of CPT. Because of the thermodynamic self-consistency the particle-hole symmetry is already broken in the region of small U as can be seen from the nonsymmetric shape of the QDOS. The curves fall off faster on the right-hand side than on the left-hand side because the former is situated in a region of small damping (compare with Fig. 1). No additional QDOS structure is found in the peripheral regions.

B. Quasiparticle splitting in the paramagnetic region

In Sec. IV A we have demonstrated unambiguously the importance of an appropriate inclusion of the model assumptions (lattice parameter, wave-vector dependences, self-consistency) even for a qualitative analysis. Hence in the following investigation of the noncollectively ordered parameter area on the basis of the MPT these basic requirements are fully taken into account.

First of all there occurs an implicit U dependence of the self-energy caused by the self-consistency procedure. This constitutes the residual influence of the Hubbard parameter after the real and imaginary parts have been divided by U^2 and displaced in the spectrum to lower energies by the amount of the Stoner shift $\frac{1}{2}Un$. For $n = 0.25$ and various values of U this is illustrated in Fig. 4. The local contribution of the damping drawn there shows the typical $(E - \mu)^2$ behavior in the vicinity of the Fermi level for all values of the Coulomb repulsion. But there is a weak U dependence of the chemical potential giving rise to similar trends in the positions and values of the damping maxima. Their shifts are rather small but their strengths clearly differ. Correspondingly there are similar differences for the real parts. Consequently, in addition to the well-known explicit U behavior of the self-energy, there are always pronounced implicit corrections that have to be taken into account, too.

Above a certain strength of the coupling parameter (its concrete value depends on the degree of band filling) in the paramagnetic spectral density we have observed a trend towards splitting into two excitations. As an example $A_{k\sigma}$ is depicted in Fig. 5 in the vicinity of the R point for $U = 1.0$ and $n = 0.75$. Taking $\alpha = 0.6$ one clearly defined quasiparticle state just above the chemical potential is accompanied by a substantially smaller subsidiary

maximum which is produced by the complex behavior of the self-energy but does not in any way define an excitation. Going up to a slightly larger α the value of the subsidiary maximum is nearly doubled indicating the existence of a second quasiparticle state. Further raising α quickly drives the upper excitation peak into regions with small imaginary part of the self-energy where its lifetime increases remarkably. On the other hand, the lower quasiparticle is broadened due to an enlarged damping at the R point.

Logically there arises the question whether the upper peak corresponds to a well-defined quasiparticle or whether it is only a special damping effect. Therefore we have looked for the solutions of the equation (2.14) which define the excitation energies. The resulting paramagnetic quasiparticle band structure is exhibited in Fig. 6 along different directions of high symmetry of the simple-cubic Brillouin zone for several coupling parameters. There is one dispersion branch which is spread over the whole Brillouin zone. It lies close to the center of gravity of the free Bloch band. Compared with the displacement of $\frac{1}{2}Un$ of a Hartree-Fock band, the residual shift of this branch is drastically reduced with increasing Coulomb
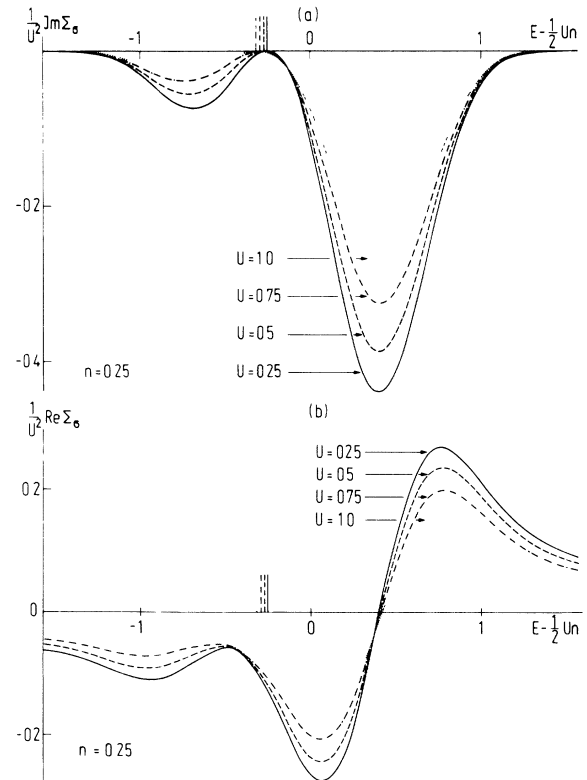

FIG. 4. Implicit U dependence of the imaginary part (a) and real part (b) of the self-energy after they have been divided by U^2 and shifted downwards in the spectrum by an amount of $\frac{1}{2}Un$. The vertical bars of the corresponding linetype determine the position of the chemical potential. It is always the local contribution of the self-energy belonging to $\mathbf{k} = \frac{1}{2}(1,1,1)$ that has been plotted.
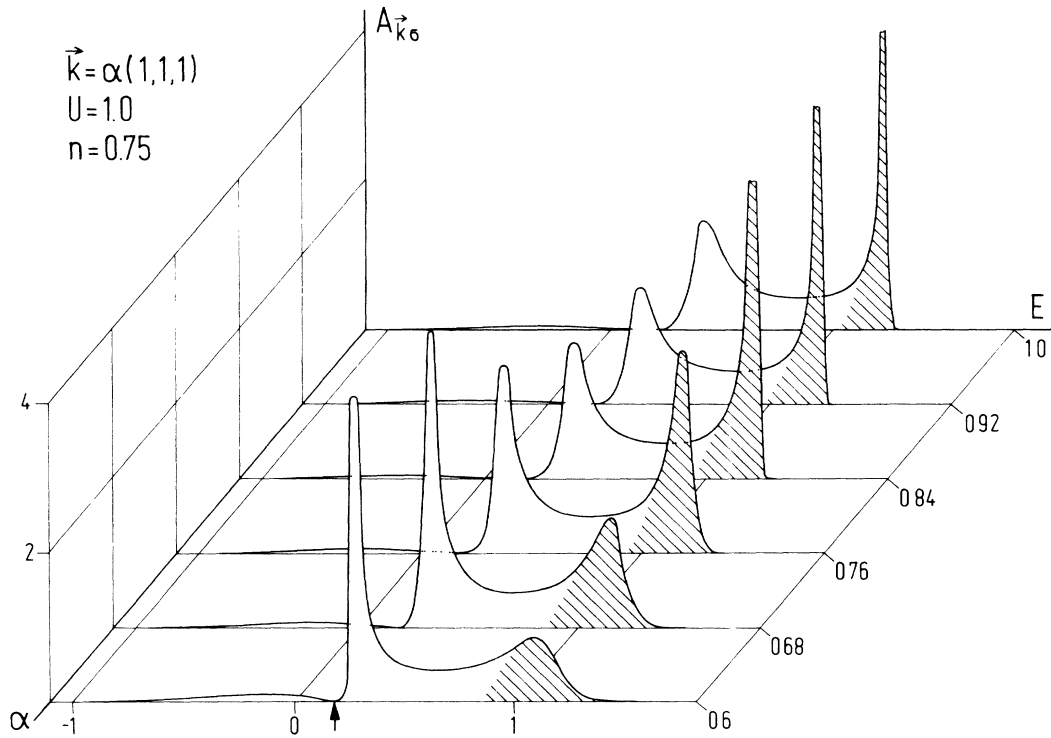
FIG. 5. Spectral density $A_{k\sigma}$ as a function of energy for several wave vectors in the neighborhood of the R point. The second quasiparticle is emphasized by the hatched areas. The other parameters are given in the plot.
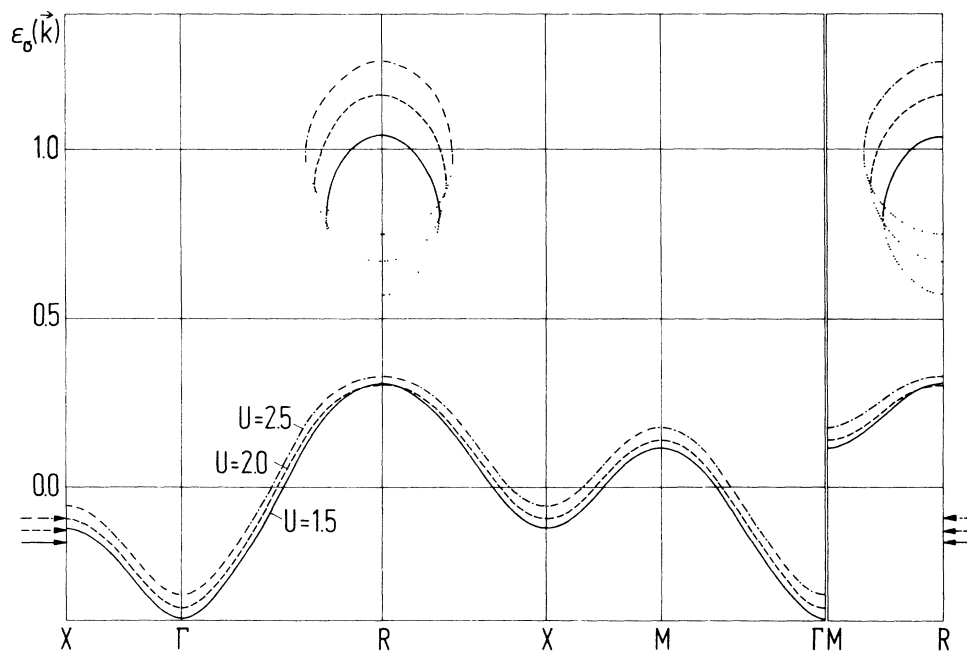

FIG. 6. Paramagnetic quasiparticle band structure along different directions of the simple-cubic Brillouin zone. Solid curve: $U = 1.5$; dashed curve: $U = 2.0$; dashed-dotted curve: $U = 2.5$. The dotted dispersion branches are mathematical solutions of (2.14) without any physical significance. The band occupation is $n = 0.25$; arrows at the margins indicate the location of the Fermi energy.

matrix element. The width of this subband is always smaller than that of the free Bloch band and it decreases slightly when U grows. Relative to the original $\varepsilon(\mathbf{k})$ the wave-vector dependence of the lower branch is distorted.

In addition to this low-lying subband further solutions of (2.14) were obtained for some wave vectors. At first they appear only in part of the Brillouin zone and not until a second critical value of U—being the larger the smaller n—is exceeded, which is not plotted here, do they extend over the whole zone. For this to happen, coupling strengths have to be chosen from the domain $U \gtrsim 1.0$. Of course, for the CPT this will be beyond its range of validity but we believe that the modified perturbation theory yields reliable results even when the electron repulsion is larger than the bandwidth. This may, e.g., be checked by comparison with findings of theories formulated for the strong-correlation regime.

The extra solutions always appear in pairs. This can formally be understood from the behavior of the real part of the self-energy. A detailed inspection shows that there always have to be one or three solutions of (2.14). But if there are three, one of it is situated in an energy region with large damping. Therefore the broadening of this excitation is so strong that it completely vanishes in the background of the spectral density, which is in accordance with the results of Fig. 5. This is to say that it is only a mathematical fixpoint of (2.14) without any physical relevance.

As the most important consequence we find the two quasiparticle subbands of the Hubbard model which are well-known from its strong-coupling limit. It is worth noting that a perturbation approach starting from the free band is able to reproduce qualitatively these two dispersion branches about T_0 and $T_0 + U$, respectively. Because we have performed a second-order perturbation theory only, it is of course not surprising that the exact position of the bands cannot be reproduced. In particular a n dependence remains in the splitting of the two subbands.

It has to be mentioned that the additional physical band first appears for wave vectors which correspond to maximal Boch energies. Here a propagating test electron has a very small group velocity and therefore is quite strongly localized. Hence it sees an "atomic Hubbard crystal" which consists only of two energy levels separated by the energy amount U. Moreover if the energy of the test electron is large, already moderate interaction parameters are sufficient to produce a second subband lying energetically above the first one. At the Γ point—another wave vector with vanishing group velocity of the test electron—an intermediate U is not strong enough to push the second subband above the first one. Hence the upper subband does not occur before U has become quite large. In other $\mathbf{k}$ regions the test electron moves fast, therefore "averages" over the two atomic situations and is similar to a Stoner-type excitation. In addition, a splitting of a band is accompanied in general by a repulsion of the subbands favoring a flattening of the lower dispersion branch.

These properties are reflected in the QDOS which we have plotted in Fig. 7 for $n = 0.25$ and various values of the Hubbard parameter. The small extensions at the sides of the QDOS are attributed to the broadening of the quasiparticles (compare Figs. 2 and 5). There is a sub-
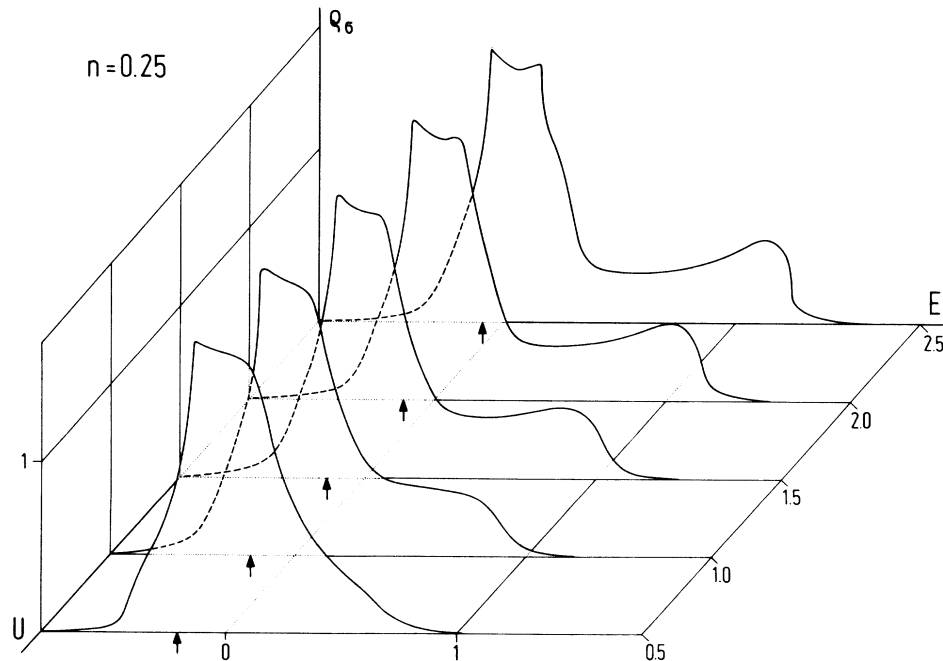

FIG. 7. Paramagnetic QDOS for $n = 0.25$ and various U values. Again the arrow indicates the position of the chemical potential.

band for all U in the vicinity of the zero of energy, the center of gravity of which changes only insignificantly when U is increased. Especially it is not shifted as much as one would expect for a Stoner-type band. This subband contains electrons which while propagating in the crystal meet predominantly empty lattice sites. Apart from that there occurs a second subband which for small U is only visible as a shoulder. It shifts proportional to the interaction parameter with a proportionality factor of roughly 0.5. This subband corresponds to quasiparticles which hop mainly via lattice sites already occupied by another one with the opposite spin which is why an additional energy of U is necessary. Because it is unlikely to find two quasiparticles at the same site for an electron number of $n = 0.25$, the weight of the upper subband is far smaller than that of the lower one. The distribution of $1 - n_{-\sigma}$ for the lower and $n_{-\sigma}$ for the upper subband, which holds exactly in the limit of infinite U, is recovered approximately. The separation of the second subband becomes more pronounced if a greater band filling is chosen. This may already be inferred from Fig. 3, but Fig. 8 provides another example for this assertion, too.

In conclusion, for nearly any band occupation n there are two quasiparticle subbands in the spectrum which are both displaced compared to the single Hartree-Fock band. The distribution of their spectral weights corresponds roughly to that obtained in the atomic limit. For instance, the QDOS obtained by the moment method of

Nolting et al.[16−19] exhibit qualitatively exactly the same features as discussed above. If it hence is possible to explain the satellite structure in the Ni spectrum in detail within the frame of a second-order perturbation formalism, this satellite is not made of propagating bound hole-hole pairs but it is rather due to single (quasi-) holes moving via lattice sites occupied by another (quasi-) hole with reversed spin. This picture is in accord with Ref. 38 where detailed calculations show an excellent agreement with experiment.

In the present approach the results for more than half-filled bands may be constructed by the particle-hole symmetry of the Hubbard model. We therefore in general deal only with the case $0 \leq n \leq 1$. Analyzing in this domain the n dependence of the QDOS for a given Coulomb repulsion shows that in empty (or completely filled) bands no electron correlations are present and the self-energies vanish identically. Then one finds the Stoner results, which are exact in this situation. Hence, when the electron or hole number is small, the effects described above are weak and almost invisible. Increasing the band occupation towards $n = 1$ strengthens more and more the tendency of building up two subbands in the QDOS even when the U values are only moderate.

C. The ferromagnetic phase transition

For certain parameter constellations there is an additional fixpoint of the equations (3.33), belonging to a fer-
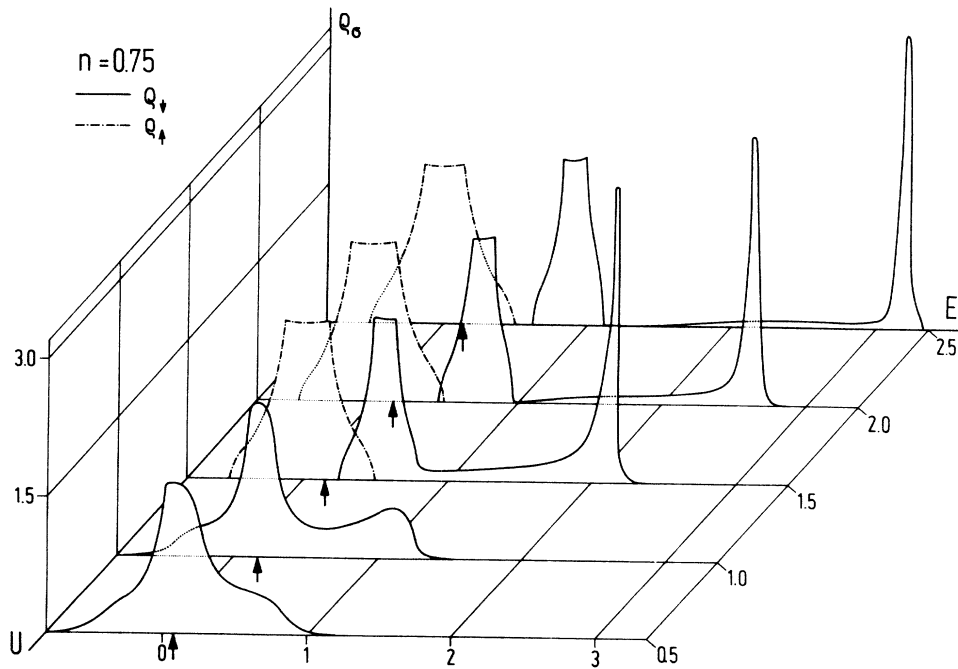

FIG. 8. Ferromagnetic QDOS for $n = 0.75$ and various Coulomb matrix elements U. Dashed curve: $\rho_\uparrow$; solid curve: $\rho_\downarrow$. The Fermi level is marked by an arrow.

romagnetic state of the system. We calculated the internal energy at $T = 0$ K, which is sufficient for answering the question of stability, for some parameter sets. In every case it turned out that the collectively ordered crystal is physically realized.

We first display the ferromagnetic QDOS in Fig. 8 for fixed band filling ($n = 0.75$) but varied Coulomb repulsion. Although the choice of $U = 2.5$ seems to be large for a perturbation theory the results are physically very plausible. The paramagnetic densities of states as repeatedly mentioned show a trend towards formation of two bands. In passing over to ferromagnetism the polarization of the conduction electrons, defined as the quotient of magnetization and mean electron number, increases abruptly to a high value close to saturation. The less electrons there are in the band the sharper this transition is. Within the scope of the obtainable numerical accuracy it was not possible to decide whether the transition is accompanied by a finite jump or a very steep but continuous ascent. In any case, taking into account the effect of finite temperatures should lead to a broadening of the transition and more accurate conclusions may be possible then.

The dashed majority-spin QDOS $\rho_\uparrow$ is identical with the Stoner density of states corresponding to a shift of $Un_\downarrow$. Because the magnetization is saturated the occupation number $n_\downarrow$ is zero and $\rho_\uparrow$ coincides with the free Bloch density of states. From a physical point of view

this reflects the fact that in a system of electrons with majority-spin direction only there is no possibility whatsoever for two electrons to experience the Coulomb interaction. In compliance therewith the system behaves like a noninteracting Fermi gas in a simple-cubic lattice. In going to finite temperatures this picture will no longer be correct because then minority-spin electrons can be excited and the Coulomb repulsion will have effects.

Even at zero temperature the situation for a spin-$\downarrow$ test electron is much more complicated because the Pauli principle is also obeyed at lattice sites which are already occupied with a majority-spin electron. Consequently the spectrum consists of two subbands. Energetically they are separated approximately by an amount of U and they are connected by a weak damping induced background contribution.

Figure 9 attests to the fact that indeed both subbands are formed by well-defined quasiparticles. It shows the ferromagnetic spin-$\downarrow$ band structure for $U = 1.5$ and 2.5. For comparison, the dispersion of Bloch electrons is also drawn as a dashed-dotted curve, made to coincide at the R point. Again there occurs a third mathematical but physically nonrelevant solution of (2.14), which is indicated by the dotted curves. Taking $U = 1.5$ the upper subband is not yet spread over the whole zone. The physical branches follow that of the Bloch electrons quite well in curvature but with a smaller bandwidth. Branches belonging together are separated approximately by an
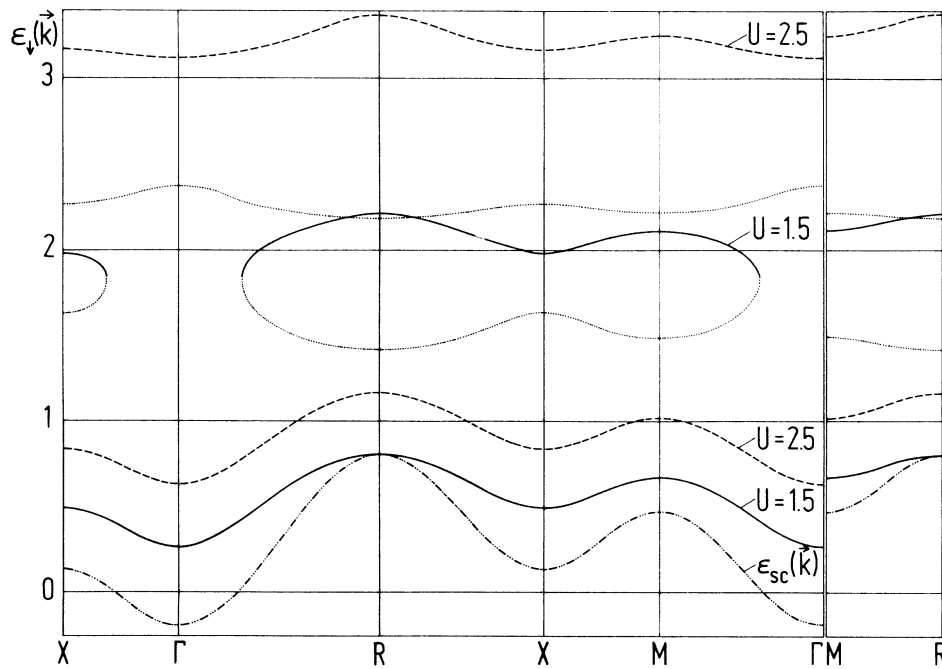

FIG. 9. Spin-$\downarrow$ ferromagnetic quasiparticle band structure in the simple-cubic Brillouin zone for $n = 0.75$. Solid curve: $U = 1.5$; dashed curve: $U = 2.5$. Dotted lines are the unphysical solutions of (2.14). The dashed-dotted line describes the dispersion of Bloch electrons, fitted at the R point.

amount of U.

The QDOS's show already that the minority-spin spectrum is shifted to higher energies in rough proportion to U. This is seen more clearly in Fig. 10 where we have plotted the difference between the lower band edge of the minority-spin spectrum and the Fermi level as a function of the Hubbard parameter U. In the Stoner model this quantity behaves like $Um = Un$ in the case of saturation magnetization. But in the present approach the slope is less than half this value. In contrast to mean-field theory where ferromagnetism is caused by a rigid shift of Um of spin-↑ versus spin-↓ single-band spectra, a somewhat different mechanism works in the MPT. It consists in a narrowing of the lower spin-↓ subband due to a lowering of the weight factor $1 - n_\uparrow$, where the occupation number $n_\uparrow$ increases from $\frac{1}{2}n$ to n in the transition region. This effect is superimposed by a displacement of the total QDOS which is proportional to U but strikingly weaker than in the Hartree-Fock case. In the paramagnetic case, that is, in a situation where the self-energies themselves are shifted as $\frac{1}{2}Un$, the position of the lower subband was nearly independent of the interaction parameter. Hence the obvious conjecture arises that the remaining displacement of the complete spectrum of the ferromagnetic solution is about $\frac{1}{2}Um$ when the self-energy is shifted by $Um \approx Un$. Following this argumentation one expects Curie temperatures which are lowered drastically in comparison with the unphysically high values of mean-field theory.

In Fig. 11 we show the phase diagram for paramagnetism and ferromagnetism at $T = 0$ K as a function of Coulomb repulsion U and band filling n. In addition the phase boundary of the Stoner model is plotted as a dashed line. Above all we recognize that the parameter region with a collectively ordered electron system is shrunk drastically in comparison with the Hartree-Fock calculations. This is not at all surprising because it is well known that the possibility of spontaneous magnetization is considerably overestimated in the mean-field theory of the Hubbard model. But the most remarkable fact is that there seems to be a lower critical band occupation $n_c \approx 0.6$ below which we have not found any ferromagnetic solutions although we went to very high U values. Of course, strictly speaking such an assertion will not be free of doubts considering that a perturbation formalism valid for weak electron-electron correlations has been used. We nevertheless believe that it is reliable in the coupling strength region plotted. In contrast the Stoner theory yields a finite $U_{St} = U_{St}(n)$ above which the ferromagnetic solution is the stable one for any band filling n.

Close to the half-filled band case the MPT gives a critical U value for ferromagnetism which is of order 1. This reflects the physical situation that in order to obtain a macroscopic magnetic moment the gain in potential ener-
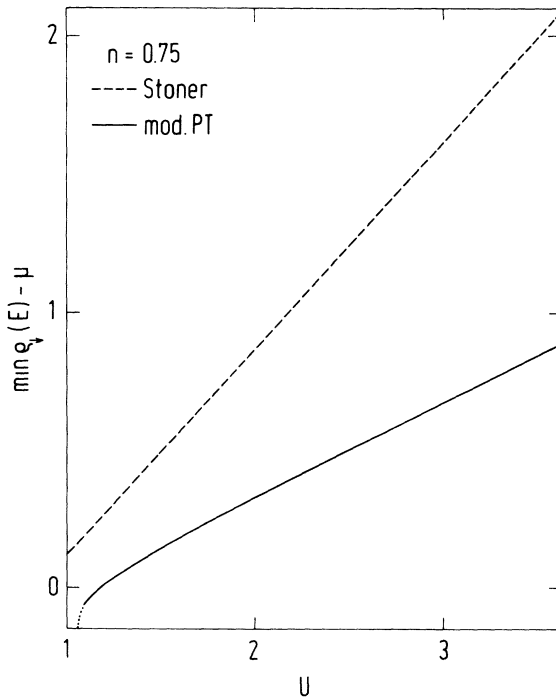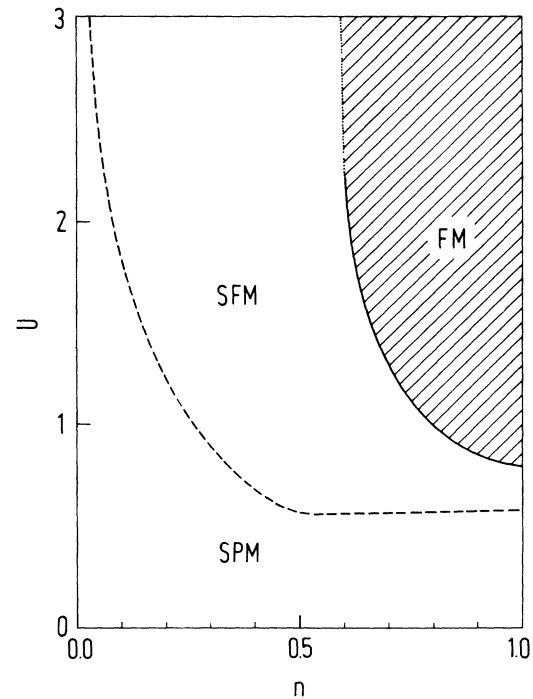

FIG. 10. Energy difference between the lower band edge of the minority-spin spectrum and the Fermi level as a function of the Hubbard parameter U at a band filling of $n = 0.75$.

FIG. 11. $T = 0$ K phase diagram para- vs ferromagnetism in terms of band occupation n and Coulomb interaction U. The hatched region corresponds to ferromagnetically ordered solutions. The dashed curve is the Stoner phase boundary, which separates Stoner paramagnetism (SPM) from Stoner ferromagnetism (SFM).

gy due to a parallel alignment of the spins which is approximately Un has to compensate at least for the loss in kinetic energy which is at most the full bandwidth $W = 1$. Hence below a coupling strength $U_c \approx 0.8$ no ferromagnetic solution occurs no matter how large or small the band filling is.

This again is in remarkable qualitative agreement with the strong-coupling phase diagram of Nolting and Borgiel.[19] The only difference is that our critical n_c is somewhat larger and our critical U_c is a little smaller than theirs. One may draw two important conclusions from this: First, the method of spectral moments, which

works particularly well in the domain of large U, is suitable even for the regime $U \approx W$ and second, it corroborates that second-order MPT is not restricted in its range of applicability to parameter constellations with $U \lesssim W$. Because of particle-hole symmetry the phase diagram for mean electron numbers $1 < n \leq 2$ is simply obtained by a reflection of Fig. 11 at the $n = 1$ axis.[39]

ACKNOWLEDGMENTS

[1]M. Gutzwiller, Phys. Rev. Lett. **10**, 159 (1963).

[2]J. Hubbard, Proc. R. Soc. London, Ser. A **276**, 238 (1963).

[3]J. Hubbard, Proc. R. Soc. London, Ser. A **277**, 237 (1964).

[4]J. Kanamori, Prog. Theor. Phys. **30**, 275 (1963).

[5]M. Cyrot, Physica B **91**, 141 (1977).

[6]T. Moriya, *Spin Fluctuations in Itinerant Electron Magnetism* (Springer-Verlag, Berlin, 1985).

[7]E. N. Economou and C. T. White, Phys. Rev. Lett. **38**, 289 (1977).

[8]E. N. Economou, C. T. White, and R. R. DeMarco, Phys. Rev. B **18**, 3946 (1978).

[9]E. N. Economou and C. T. White, Phys. Rev. B **18**, 3959 (1978).

[10]R. R. DeMarco, E. N. Economou, and C. T. White, Phys. Rev. B **18**, 3968 (1978).

[11]R. A. Tahir-Kheli and H. S. Jarrett, Phys. Lett. A **27**, 485 (1968).

[12]*Theory of Heavy Fermions and Valence Fluctuations*, edited by T. Kasuya and T. Saso (Springer-Verlag, Berlin, 1985).

[13]P. W. Anderson, Science **235**, 1196 (1987).

[14]M. Heise and R. J. Jelitto, Z. Phys. B **25**, 381 (1976).

[15]M. Heise and R. J. Jelitto, Z. Phys. B **26**, 177 (1977).

[16]W. Nolting, Z. Phys. **255**, 25 (1972).

[17]W. Nolting, Z. Phys. **265**, 173 (1973).

[18]G. Geipel and W. Nolting, Phys. Rev. B **38**, 2608 (1988).

[19]W. Nolting and W. Borgiel, Phys. Rev. B **39**, 6962 (1989).

[20]K. A. Chao, R. Kishore, and J. C. da Cunha Lima, J. Phys. C **11**, L953 (1978).

[21]R. Kishore, Phys. Rev. B **35**, 6854 (1987).

[22]H. Mori, Prog. Theor. Phys. **33**, 432 (1965).

[23]H. Mori, Prog. Theor. Phys. **34**, 399 (1966).

[24]G. Tréglia, F. Ducastelle, and D. Spanjaard, J. Phys. (Paris) **41**, 281 (1980).

[25]G. Tréglia, F. Ducastelle, and D. Spanjaard, Phys. Rev. B **21**, 3729 (1980).

[26]G. Tréglia, F. Ducastelle, and D. Spanjaard, Phys. Rev. B **22**, 6472 (1980).

[27]G. Tréglia, F. Ducastelle, and D. Spanjaard, J. Phys. C **14**, 4347 (1981).

[28]G. Tréglia, F. Ducastelle, and D. Spanjaard, J. Phys. (Paris) **43**, 341 (1982).

[29]C. Guillot, Y. Ballu, J. Paigné, J. Lecante, K. P. Jain, P. Thiry, R. Pinchaux, Y. Pétroff, and L. M. Falicov, Phys. Rev. Lett. **39**, 1632 (1977).

[30]C. S. Wang and J. Callaway, Phys. Rev. B **15**, 298 (1977).

[31]R. Taranko, E. Taranko, and J. Malek, J. Phys. F **18**, L87 (1988).

[32]L. Kleinman, Phys. Rev. B **19**, 1295 (1979).

[33]L. Kleinman and K. Mednick, Phys. Rev. B **24**, 6880 (1981).

[34]R. Taranko and E. Taranko, Physica B **153**, 232 (1988).

[35]G. Bulk and R. J. Jelitto, Phys. Lett. A **133**, 231 (1988).

[36]The question which phase is in fact the stable one cannot be answered by analyzing para-, ferro-, and antiferromagnetism only. Moreover one has—for instance—to compare with arbitrary ordered states of spin-density-wave type, which was done elsewhere by one of us on the basis of the most general single-particle approach to the Hubbard model [R. J. Jelitto, Phys. Status Solidi B **147**, 391 (1988)].

[37]R. J. Jelitto, J. Phys. Chem. Solids **30**, 609 (1969).

[38]W. Nolting, W. Borgiel, V. Dose, and Th. Fauster, Phys. Rev. B **40**, 5015 (1989).

[39]We have carried out further numerical calculations which offer interesting additional details. Though this material is too lengthy to be given here, it is available from the authors.